*Proceedings of The Twelfth (2002) International Offshore and Polar Engineering Conference*
*Kitakyushu, Japan, May 26−31, 2002*

*ISBN 1-880653-58-3 (Set); ISSN 1098-6189 (Set)*

# Dynamic Positioning of a Pipeline Launching Barge

*E. A. Tannuri and C.P.Pesce*
Escola Politécnica , University of São Paulo, São Paulo, Brazil
*G. S. Alves, I. Masetti and P.P. Ribas Ferreira*
Petrobrás, Rio de Janeiro, Brazil
*C.H. Umeda*
IPT - Research Technological Institute, São Paulo, Brazil

## ABSTRACT

This works deals with the analysis of a Dynamic Positioning (DP) system to be installed in an already existing pipeline-laying barge. In order to feed a numerical simulator, small-scale model experiments have been carried out, addressing either current as well 'wind' forces and moment. Two laying conditions have been considered: S-Lay, for intermediate deep waters and J-Lay, for deeper waters, up to 1000 meters. Numerical simulation uses a complete and validated model taking into account current (at low speed and large drift angles), waves (including current interaction) and gust wind forces. The controller has been designed using a simple nonlinear approach with thrusters dynamics included. Thrust allocation is also implemented, power being minimized by means of a pseudo-inverse matrix algorithm. Thruster failure analysis is also covered and discussed.
KEY WORDS: Dynamic positioning, pipeline launching, barge, towing tank experiments.

## INTRODUCTION

BGL1 is a crane and pipe-laying barge (Fig.1), operating in Brazilian waters for more than 20 years. Equipped with a conventional mooring system and operated with the aid of anchor handling tugboats, BGL1 was originally designed for shallow and intermediate depths. Pipe-laying has been successfully accomplished through the so-called S-Lay operation. BGL1 S-Lay is done from a stern launching ramp, positioned at starboard, with or without a *stinger* (Fig.2). Pipeline is welded on deck. Traction is sustained by means of a traction-controlling machine, of the caterpillar type.

With increasing depths, the conventional mooring positioned laying operation presents serious technical and economical limitations. S-Lay mode of operation is appropriate for shallow and intermediate depths. For deeper waters the so-called J-Lay launching is a recommended practice (Fig.3). A robust DP system can then improve position control ability, for both S- or J-Laying modes, with no loss of safety, enhancing operational time schedule and making the operation economically feasible.

Fig.1. BGL1 with a supply boat at portside.

This works deals with the analysis of a Dynamic Positioning System (DPS), to be designed in order to equip BGL1. The main goal of the present study is to determine the required power for the DPS. Both laying conditions have been addressed: S-Lay, for intermediate deep waters and J-Lay, for deeper waters, up to 1000 meters. S-Lay comprises the use of a stinger, whose effect has been properly considered. In order to feed a numerical simulator, towing tank small-scale model experiments have been carried out. Current forces and moment coefficients have been measured. 'Wind' forces and moment were experimentally determined from upside-down model towing tank tests. Numerical simulation uses a complete and validated model that takes into account current (at low speed and large drift angles), waves (including current interaction), gust wind forces and thrusters dynamics. The controller has been designed using a feedback linearization approach. Thrust allocation is implemented according Sørdalen (1997), minimizing power by means of a pseudo-inverse matrix algorithm. An example is presented for a given matrix of environmental conditions and results include a delivered power polar diagram, constructed with respect to the launching direction. Thruster failure analysis is also covered and discussed.

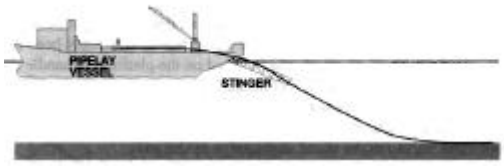


Fig.2. S-lay launching operation (adapted from Bray, 1998)

Fig.3. J-lay launching operation (adapted from Bray, 1998)

Brink and Chung (1980) developed a similar work with the utilization of simulation analysis in the design of offshore operations supported by DPS. The authors developed a complete simulator of a 30,000tons ship during ocean mining operations, including also sensors models and pipe and buffer dynamical effects. With the simulator, the authors could analyze the performance of the system, the effect of ship velocity in the operation, thruster failure consequences, performance during emergency stop, etc…

## BARGE DATA AND OPERATIONAL CONDITIONS

BGL1's main particulars are presented in Table 1.

Table 1. BGL1 main data

| | |
|---|---|
| Length (L) | 121.9 m |
| Beam (B) | 30.48 m |
| Draft (T) | 5.18 m |
| Position of CG ($x_G$) | -4.18m |
| Mass (M) | 17177ton |
| Surge Added Mass ($M_{11}$)* | 1717ton |
| Sway Added Mass ($M_{22}$)* | 8588ton |
| Yaw Added Mass ($M_{66}$)* | $1.28.10^7$ ton.m$^2$ |
| Lateral Area ($A_L$) | 1500m$^2$ |
| Frontal Area ($A_F$) | 420m$^2$ |

* at low frequency

For the S-lay operation, a constant force of 900kN applied by the pipe, acting in the backward direction at the end of the stern ramp has been considered. A smaller force of 200kN has been considered for the J-lay mode analysis. Such a force is applied to an anchoring point at a not yet existing moon-pool. The direction of this latter force (launching direction) may change within a sector of ±90°. Fig. 4 shows either applied force. For simplicity, the dynamics of the traction control machine was not modeled, the forces being ideally considered as constant.

Thrusters' position is shown in Fig.5. The system consists of three fore-body units and three stern ones. These positions were determined by layout constraints.

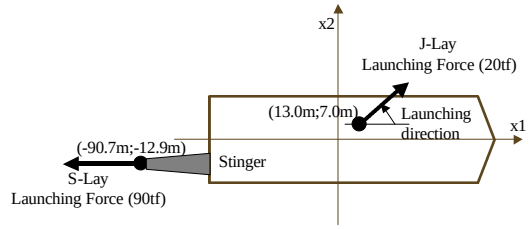


Fig.4. Launching operation. Pipeline applied forces (S-lay and J-lay)

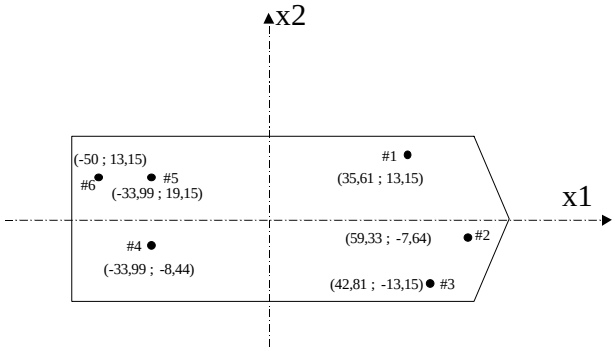


Fig.5. Propeller Positions in meters (related to $x_1x_2$ axis centered at CG)

The main requirement for the controller is the ability to keep the barge at a pre-set position during launching operation, within a maximum error of 7.5m. Moreover, the DPS must be able to maintain barge positioning even in the case of failure or maintenance of one or two thrusters, during a J-lay operation. Simultaneous inactivity due to failure or maintenance purposes is considered for pairs of thrusters, powered by the same electric control panel, namely: pairs 1-5, 2-4 and 3-6.

The threshold sea-state for the pipe laying was defined as 1.2m/s current, 12m/s wind (10min average) speed and waves with 2.0m significant height and 6.0 seconds zero up-crossing wave period.

## MODELING, SIMULATION AND CONTROL

Fig. 6 shows the simulator block diagram. Barge dynamics is simulated in the horizontal plane, according to Tannuri, Donha and Pesce (2001). The following dynamic model gives horizontal motions of the barge:

$$\begin{aligned}
&(M+M_{11})\ddot{x}_1-(M+M_{22})\dot{x}_2\dot{x}_6-M_{26}\dot{x}_6^{\,2}=F_{1E}+F_{1O}+F_{1T};\\
&(M+M_{22})\ddot{x}_2+M_{26}\ddot{x}_6+(M+M_{11})\dot{x}_1\dot{x}_6=F_{2E}+F_{2O}+F_{2T};\\
&(I_z+M_{66})\ddot{x}_6+M_{26}\ddot{x}_2+M_{26}\dot{x}_1\dot{x}_6=F_{6E}+F_{6O}+F_{6T}.
\end{aligned} \quad (1)$$

where $I_z$ is the moment of inertia about the vertical axis; $F_{1E}$, $F_{2E}$, $F_{6E}$ are surge, sway and yaw environmental loads (current, wind and waves), $F_{1O}$, $F_{2O}$, $F_{6O}$ are operation forces and moment due to the pipe being launched and $F_{1T}$, $F_{2T}$, $F_{6T}$ are forces and moment delivered by propulsion system. The variables $\dot{x}_1$, $\dot{x}_2$ and $\dot{x}_6$ are the midship surge, sway and yaw absolute velocities.

Static current forces and moment were evaluated using the experimental coefficients ($C_X$, $C_Y$ and $C_M$) defined as:

$$F_{1C}=\frac{1}{2}C_X\,\rho LTU^2;\ F_{2C}=\frac{1}{2}C_Y\,\rho LTU^2;\ F_{6C}=\frac{1}{2}C_M\,\rho L^2TU^2 \quad (2)$$

where $F_{1C}$ and $F_{2C}$ are surge and sway forces, $F_{6C}$ is yaw moment, $\rho$ is water density and $U$ is the barge velocity, relative to the water.

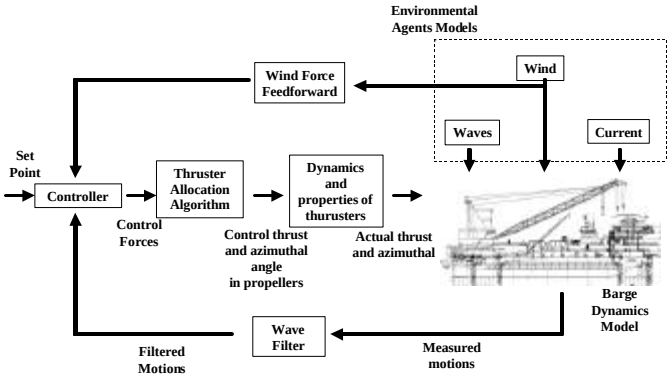


Fig.6.Simulator's block diagram

The coefficients, obtained in IPT (Research Technological Institute) towing tank, are presented in Fig.7. Viscous effects in surge coefficient were extrapolated to real scale, due to their dependence on Reynolds Number, following Simos et al (2001).

Experiments were conducted with and without the stinger model, not used in J-lay operations. For the S-Lay mode, with the stinger attached, experiments were conducted with (1%) and without trim angle. A 1% stern trim is typical for S-Lay operation. The differences between coefficients in both configurations are small, and did not affect the DPS design.

Current forces and moments associated with barge yaw rotation were evaluated using a cross-flow model presented in Simos et al. (2001).

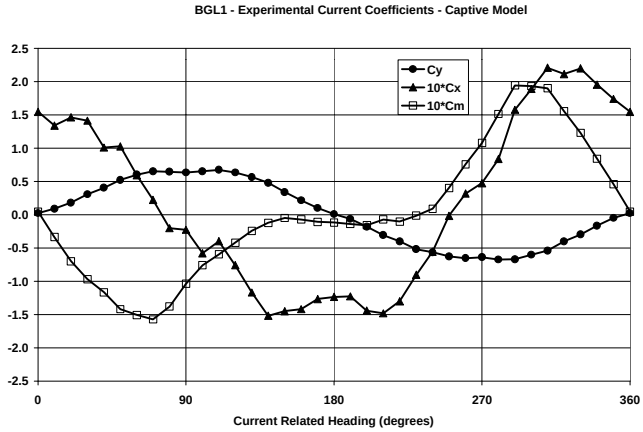


Fig.7. BGL1 Experimental Current Coefficients – S-lay operation without trim angle.

Static wind forces were also evaluated using experimental coefficients ($C_{XV}$, $C_{YV}$ and $C_{MV}$) obtained in a captive 'wind' test conducted, with the barge model superstructure turned upside down into the towing tank (Fig.8).

Wind coefficients, defined in the standard way by,

$$F_1^V = \frac{1}{2} C_{XV}\, r_a A_F V^2 ; F_2^V = \frac{1}{2} C_{YV}\, r_a A_L V^2 ; F_6^V = \frac{1}{2} C_{MV}\, r_a A_L L V^2 \quad (3)$$

are presented in Fig.9. $F_1^V$ and $F_2^V$ are surge and sway components of the wind force, $F_6^V$ is the wind yaw moment; $r_a$ is air density; $V$, the mean 'wind' velocity.

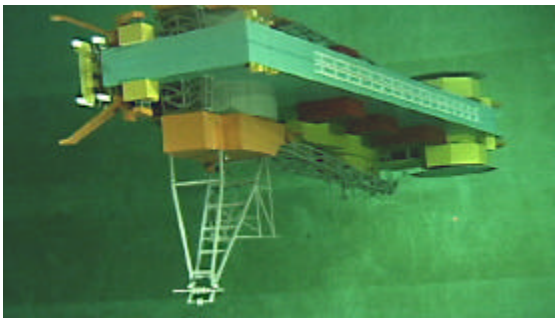

Fig.8: BGL1 Model in the"wind" loading test (model turned upside down into the water).

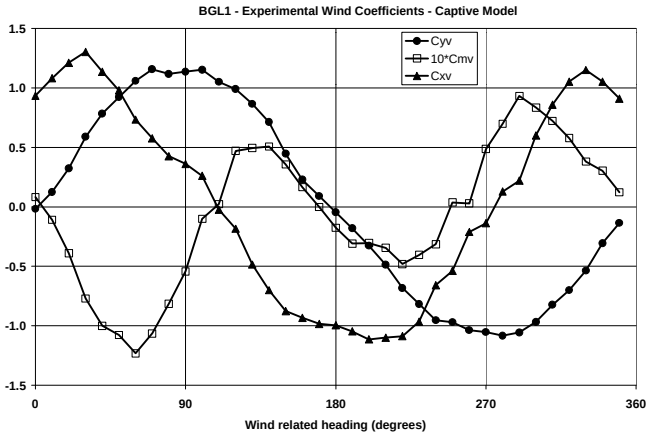


Fig.9. BGL1 Experimental Wind Coefficients

Gust spectrum simulations considered Harris-DNV formula, given by

$$S_V(w) = 1146.C.V.\left[2 + \left(\frac{286w}{V}\right)^2\right]^{-\frac{5}{6}} \quad (4)$$

where $w$ is the frequency of wind oscillation, $S_v(w)$ is the spectral density and $C$ is a surface drag coefficient, used as 0.0015 for moderate seas. Fig. 10 shows time series of wind velocity, for a mean wind velocity of 12m/s, as is the case in the present analysis.

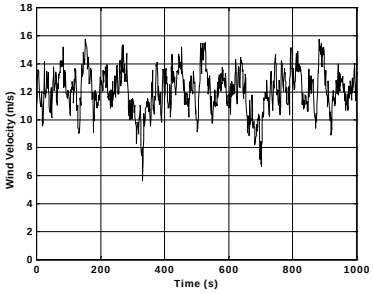


Fig.10. Wind speed using the Harris-DNV gust spectrum

A Pierson-Moskowitz wave spectrum was adopted, and mean drift wave forces were evaluated using the drift coefficients obtained from a very well known and validated wave-body interaction computer code[1].

[1] WAMIT

Fig.11 presents an illustrative example of such coefficients for a 30° wave-heading angle. Second order slow drift forces were evaluated using Aranha and Fernandes (1995). Current-wave interaction effect on wave drift forces is estimated following Aranha (1996). First order wave forces are not included in the model.

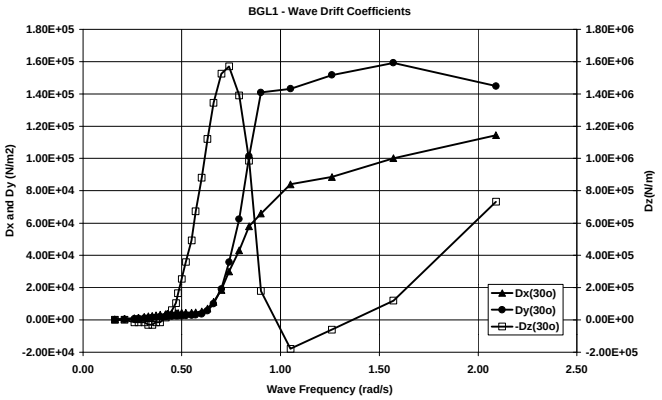


Fig.11. BGL1 Wave Drift Coefficients for 30° wave heading angle

Besides the environmental forces, the simulator presents a model for propeller dynamics, in order to evaluate the lag between the controller demand and the propeller response. The model also gives an estimate of total power consumed by each thruster.

As already explained, the barge will be equipped with 6 azimuth ducted thrusters. For simulation purposes, a series Ka propeller with a 19A nozzle, with 2m diameter and 1.6m pitch has been used. The torque ($K_Q$), thrust ($K_T$) and nozzle ($K_{TN}$) coefficients are given by Lewis (1988) and presented in Fig.12.

Drive system efficiency of each thruster is 80%, and the efficiency curves, here defined as the delivered thrust (kN) divided by the power (kW), are presented in Fig.13, for two different inlet velocities. The maximum power of each unit is 1650kW, resulting in a maximum values for the thrust of 290kN for 1.2m/s inlet velocity and 330kN for 0.5m/s.

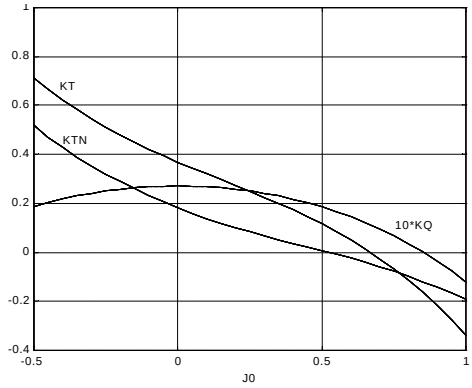


Fig.12. Propeller coefficients $K_T$, $K_Q$ and $K_{TN}$ as a function of advance coefficient $J_0$

The electrical dynamics of the thruster controller was disregarded, since its time constant is about 50ms, negligible compared to the mechanical one (about some seconds). Therefore, a simplified model was used for all these sub-systems, disregarding the electrical dynamics. Hansen et al. (2000) showed that this model can accurately predict force and power consumption in the thrusters. Model parameters were adjusted so that it takes approximately 15s for the thruster to raise from 0kN to 290kN (Fig.14). As usual, the dynamics of thrusters was not taken into account in the design of the controller.

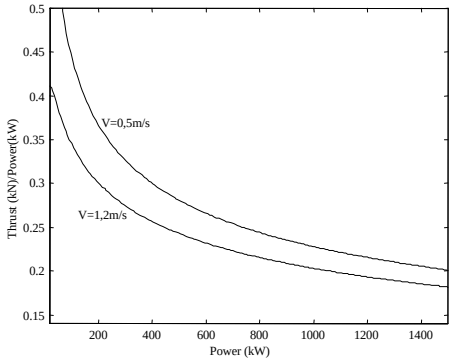


Fig.13. Efficiency curves for propeller series Ka

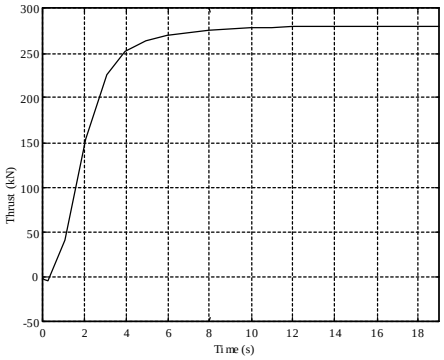


Fig.14. Efficiency curves for propeller series Ka

The thruster allocation algorithm is based on a modified pseudo-inverse technique, by Sørdalen (1997), and is presented in Appendix A.

Power analysis in most existing procedures is usually done for static equilibrium only, considering several environmental conditions and "allocating" the thrust delivered by the propellers to counteract the static force. Then, some critical cases are simulated dynamically. Some correction may be included in the power if the vessel response is not satisfactory, as is, for example, the case when thrust saturation is reached. In the present work, the analysis under an environmental condition matrix was done directly, through dynamic simulations. Such a choice implied the use of a simple control algorithm requiring few parameters to adjust.

A feedback linearization controller (Slotine and Li, 1991) was implemented in the simulator, based on the "inverse" of the non-linear dynamics of the barge; it is presented in Appendix B. This is, obviously, an "ideal" technique, which may induce some practical implementation problems, mainly related to modeling robustness error [2]. Nevertheless, this procedure allows predicting the dynamical solicitation of each thruster to counteract environmental force oscillations. The reference point for the controller is the corresponding launching point for S-lay or J-lay operation (Fig.3). A feedforward controller was designed to counteract wind forces.

[2] An extra term can be used to increase controller robustness of the controller, resulting in a sliding mode control (Tannuri, Donha and Pesce, 2001)

SIMULATIONS

## S-Lay Operation

In the S-lay operation, a 90ton force is applied to the stinger, requiring a large amount of counteracting power to deal with it and with the environmental forces. Collinear incidence of waves, wind and current was considered, direction varying from $0^o$ to $345^o$, within a $15^o$ discretization. The results of the dynamical simulations were analyzed and power polar plots were constructed. Stern thrusters 4, 5 and 6 delivered the largest forces in almost all cases. Fig. 15 presents a polar diagram for the thruster number 6.

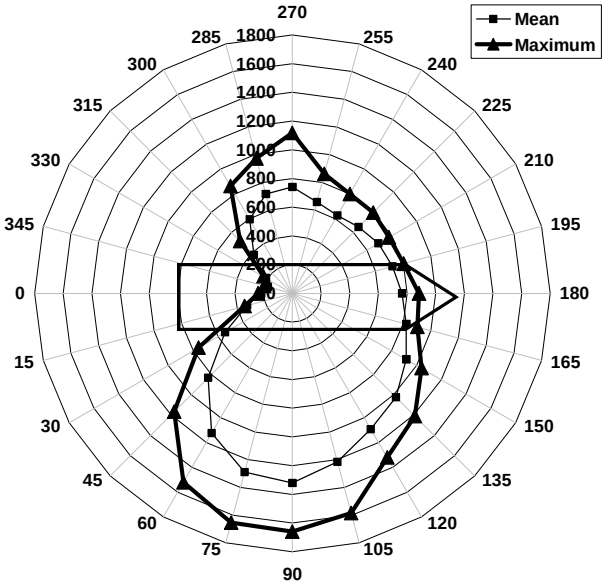


Fig.15. S-Lay – Power delivered to thruster 6 (kW) – polar plot

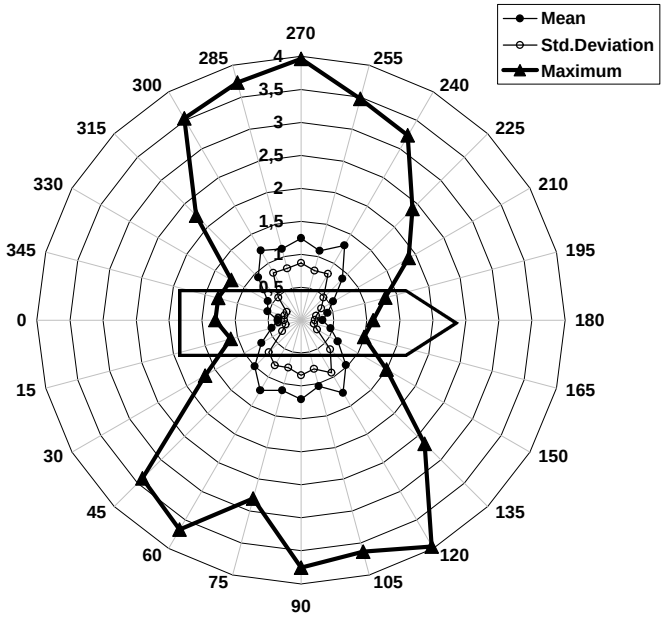


Fig.16. S-Lay – Displacement of lauching point (meters) – polar plot

As can be noticed, the saturation value is reached for environmental incidence between $75^o$ and $90^o$. However, positioning requirement is respected for all incidences, as can be seen in Fig.16, a polar plot showing the displacement of the reference point, during operation. The critical cases are beam incidence ($90^o$ and $270^o$) and bow ($120^o$) incidence, implying a maximum displacement of 4.0m. The maximum allowable displacement, for S-lay operation, is assumed to be 7.5m.

The total power delivered by the DPS is presented in Fig.17. Again, beam sea incidence is the most critical one, requiring approximately 7000kW to perform the operation.

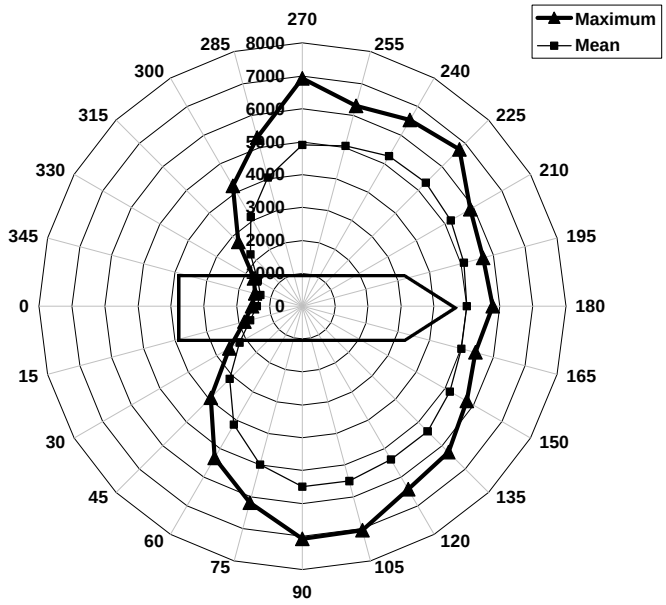


Fig.17. S-Lay - Total power (kW) – polar plot

Time simulations for the critical case ($90^o$ incidence) are shown in the next figures. Fig. 18 presents the trace plot of the barge and the mean azimuth thrusters directions, as well as the reference point trace. As expected, sway oscillation is the most important one, presenting a motion of approximately 4m away from the set-point position.

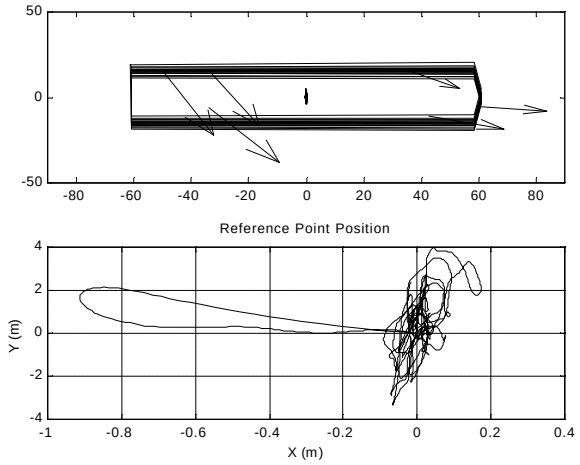


Fig.18. S-Lay – Trace plots for $90^o$ incidence

Fig.19 presents time series of the reference point position and yaw angle, which keeps values smaller than $1^o$, during the whole simulation.

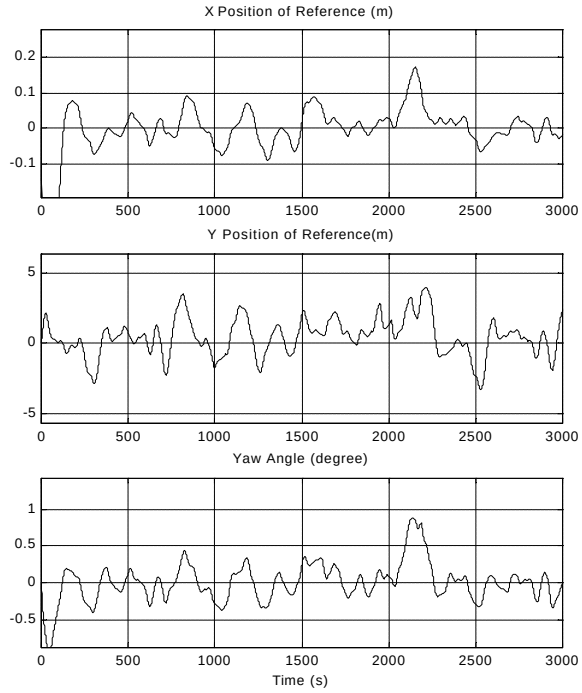


Fig.19. S-Lay –Reference position and yaw angle time series for 90$^o$ incidence

Finally, power consumption for each propeller is presented in Fig.20, confirming that stern thrusters are the most required ones. In this case saturation is reached at $t$=2115 seconds.

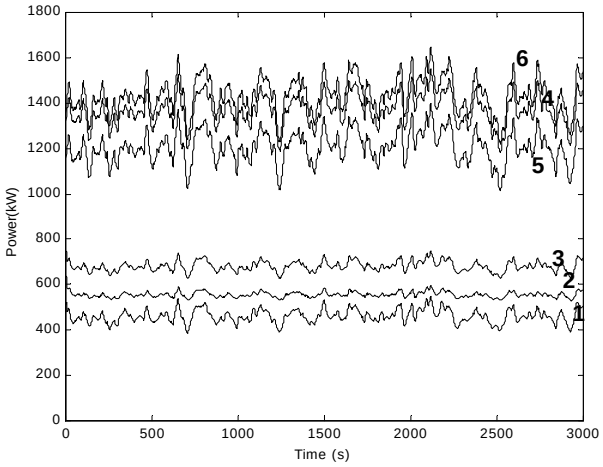


Fig.20. S-Lay – Power consumption in thrusters time series for 90$^o$ incidence

## J-Lay Operation

DPS analysis allows the designer to determine the best position the J-lay launching system should be installed, from the point of view of required power. Two options were considered: at a midship "moon-pool", shown in Fig.4, or at a stern structure, located at (x= -65.9m;y=10.3m). Three laying directions (90$^o$, 180$^o$ and 270$^o$) were analysed for both options, considering 24 collinear environmental directions (between 0$^o$ and 345$^o$). The plot for the maximum individual thruster power is shown in Fig.21, for the critical laying direction of 90$^o$.

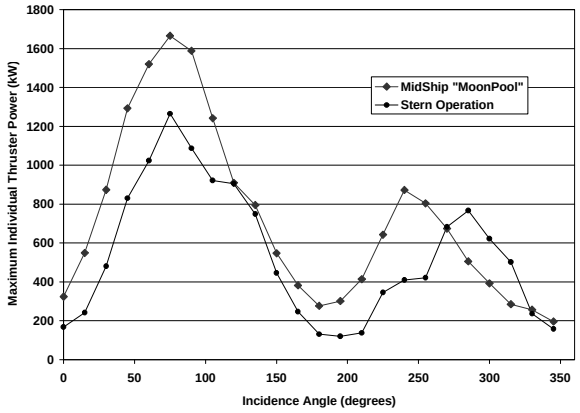


Fig.21. J-Lay – Maximum individual power (no thruster failure)

The stern operation introduces a 20t force applied to the stern. The thrusters at bow are less required than the stern ones, what introduces a lack of balance to the system. For example, for 75$^o$ incidence direction thruster number 6 saturates and the difference registered in the delivered power between stern (4, 5 and 6) and bow (1, 2 and 3) thrusters are shown in Fig.22 and Fig.23.

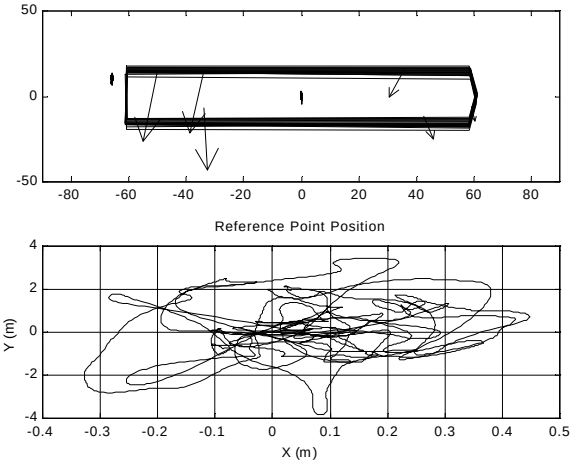


Fig.22. J-Lay – Trace plots for 90$^o$ incidence and 75$^o$ launching direction – stern operation

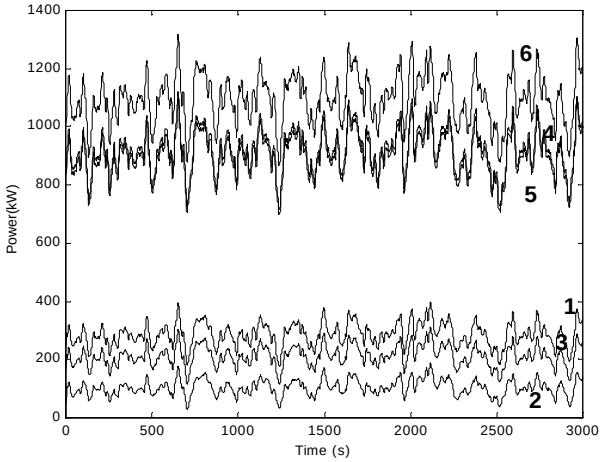


Fig.23. J-Lay – Power consumption in each thruster time series for 90$^o$ incidence and 75$^o$ launching directions – stern operation

Fig.24 and Fig.25 refer to the conditions applied to the midship J-lay configuration. Power is well distributed among all thrusters. Individual power consumption is smaller in stern thrusters compared to the values attained during a stern operation.

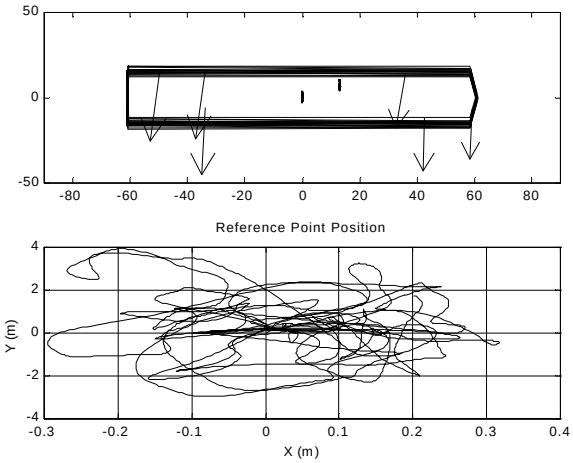


Fig.24. J-Lay – Trace plots for 90$^o$ incidence and 75$^o$ launching direction – Moonpool operation

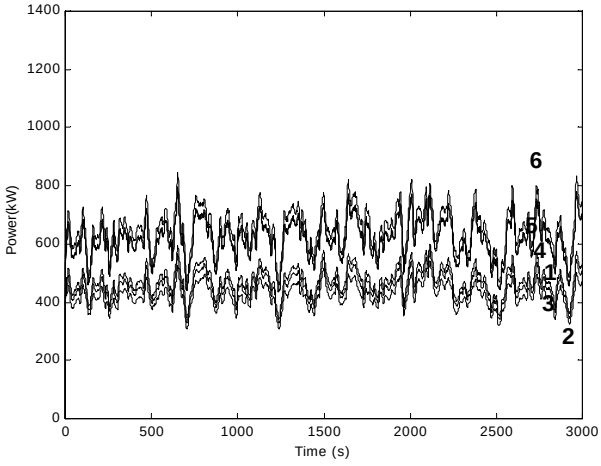


Fig.25. J-Lay – Power consumption in each thruster time series for 90$^o$ incidence and 75$^o$ launching direction – Moonpool operation

As can be inferred from the previous analysis, a possible failure in any stern thruster turns the stern J-Lay operation unfeasible. In such a situation barge position cannot be kept inside the 7.5m maximum allowable oscillation. Differently, for midship (moon-pool) J-Lay configuration, operation turns to be feasible even in the event of failure of one stern and one fore-body thruster. The critical case corresponding to a 75$^o$ environmental incidence is shown in Fig. 26 and Fig.27, when thrusters 6 and 3 are inactive. Power consumption is redistributed among the remaining active propellers and the reference point is kept inside the 7.5m maximum allowable excursion around the set point.

The simulations performed here considered a fixed set-point position. During the operation, however, set-point is not constant, because the barge must follow a pre-defined path. Since pipe laying normally is executed at low speed, the power required to perform the path-following operation is approximately the same as the fixed set-point analyses. Some results on path-following control applied in the some case can be found in Tannuri and Pesce, (2002).

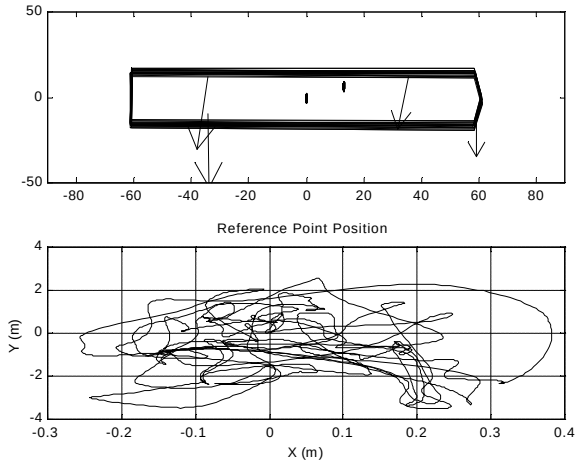


Fig.26. J-Lay – Trace plots for 90$^o$ incidence and 75$^o$ launching direction – Moonpool operation and thrusters 3 and 6 inactives

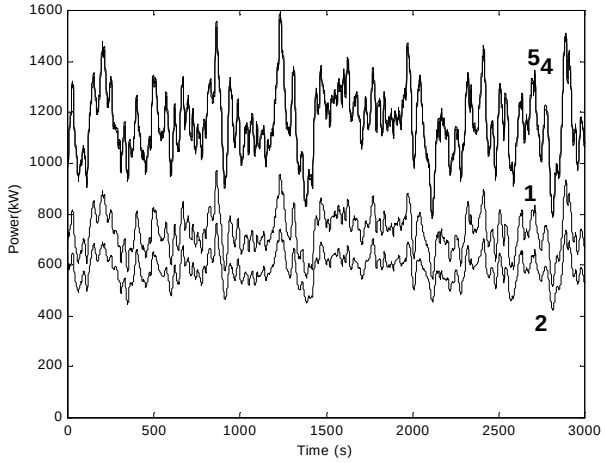


Fig.27. J-Lay – Power consumption in each thruster time series for 90$^o$ incidence and 75$^o$ launching direction – Moonpool operation and thrusters 3 and 6 inactive

## CONCLUDING REMARKS

A comprehensive and up-to-date case-study analysis of a Dynamic Positioning System to be installed in an already existing pipeline-laying barge has been successfully carried out. In order to feed a numerical simulator, small-scale model experiments have been conducted, addressing either current as well 'wind' forces and moment. Two laying conditions have been considered: S-Lay, for intermediate deep waters and J-Lay, for deeper waters, up to 1000 meters. Numerical simulation used a complete and validated model taking into account current (at low speed and large drift angles), waves (including current interaction) and gust wind forces. The controller was designed using a simple nonlinear approach with thrusters dynamics included. Thrust allocation was also implemented, power being minimized by means of a pseudo-inverse matrix algorithm. Propeller failure analysis was carried out. Saturation occurs for some environmental and incidence angle conditions. For S-Lay mode, power saturation value is reached in propeller number 6, for environmental incidence between 75$^o$ and 90$^o$. However, positioning requirement is respected for all incidences. From the other side, a possible failure in any stern thruster turns the stern J-Lay operation unfeasible. In such a situation barge position cannot be

kept inside the 7.5m maximum allowable oscillation. Conversely, for the midship (moon-pool) J-Lay configuration, operation turns to be feasible even in the event of failure of one stern and one fore-body thruster, as it should be expected.

## ACKNOWLEDGMENTS

This work has been supported by Petrobras and the State of São Paulo Research Foundation (FAPESP – Process no. 98/13298-6). A CNPq/CTPETRO research grant, process no. 469095/00, is also acknowledged. The authors thank Mr. R. Pesce for helping with simulations and diagrams.

## REFERENCES

Aranha, J.A.P., Fernandes, A.C. (1995), "On the second-order slow drift force spectrum", Applied Ocean Research, vol. 17, pp.311-313.

Aranha, J.A.P. (1996), "Second order horizontal steady forces and moment on a floating body with small forward speed", Journal of Fluid Mechanics, vol 313.

Bray, D., (1998), "Dynamic Positioning", The Oilfield Seamanship Series, Volume 9, Oilfield Publications Ltd. (OPL).

Brink, AW, and Chung, JS (1980, 1982). "Automatic Position Control of a 30,000 Ton Ship Mining Systems," Proc Offshore Technology Conf, Houston, 1980, co-authored with A.W. Brink; also in ASME Trans. *J Energy Resources Technology*, 1982.

Hansen, J.F., Lauvdal, T., Ådnanes, A.K., "Modeling and Simulation of Variable Speed Thrusters Drives with Full-Scale Verification", Proceedings of the 5th IFAC Conference on Maneuvering and Control of Marine Crafts (MCMC), Denmark, 2000.

Simos, A.N., Tannuri, E.A., Pesce, C.P. and Aranha, J.A.P. (2001): "A quasi-explicit hydrodynamic model for the dynamic analysis of a moored FPSO under current action", Journal of Ship Research, Vol.45, No.4, pp289-301.

Slotine, J.J.E., Li, W., "Applied Nonlinear Control", Prentice Hall, New Jersey, 1991.

Sørdalen, O.J. (1997), "Optimal Thrust Allocation for Marine Vessels", Control Engineering Practice, Vol.5, No.9, pp1223-1231.

Tannuri, E.A., Donha, D.C., Pesce, C.P. (2001), "Dynamic positioning of a turret moored FPSO using sliding mode control", International Journal of Robust and Nonlinear Control, Vol.11, Issue 13, pp1239-1256.

Tannuri, E.A., Pesce, C.P. (2002), "Comparing two different control algorithms applied to dynamic positioning of a pipeline launching barge", submitted to 10th Mediterranean Conference On Control And Automation.

## APPENDIX A– THRUSTER ALLOCATION LOGIC (TAL)

Being $\mathbf{T} = \begin{pmatrix} T_{x1} & ... & T_{xn} & T_{y1} & ... & T_{yn} \end{pmatrix}^T$ the vector containing the surge ($x$) and sway ($y$) components of forces of the $n$ azimuth thrusters and $\mathbf{F_T} = \begin{pmatrix} F_{1T} & F_{2T} & F_{6T} \end{pmatrix}^T$ the resulting surge and sway forces and yaw moment of thrusters. TAL objective is to determine $\mathbf{T}$ in order to make the resulting vector $\mathbf{F_T}$ approximately equal to the controller commanded forces, with minimum fuel consumption. A simple relation between $\mathbf{T}$ and $\boldsymbol{\tau}$ can be derived:

$$\mathbf{AT} = \mathbf{F_T} \quad \text{where} \quad \mathbf{A} = \begin{pmatrix} 1 & .. & 1 & 0 & .. & 0 \\ 0 & .. & 0 & 1 & .. & 1 \\ -y_1 & .. & -y_n & x_1 & .. & x_2 \end{pmatrix} \qquad (5)$$

being $(x_i, y_i)$ the position of azimuth thruster $i$ in $xy$ coordinate system. Due to redundancy, $\mathbf{A}$ is a non-square matrix, and several values of $\mathbf{T}$ satisfy Eq.(6). Since the fuel consumption is approximately proportional to the square of the force delivered by each thruster, the solution with minimum $\|\mathbf{T}\|_2$ is given by:

$$\mathbf{T} = \mathbf{A}^T (\mathbf{A}\mathbf{A}^T)^{-1} \mathbf{F_T} \qquad (6)$$

where $\mathbf{A}^T (\mathbf{A}\mathbf{A}^T)^{-1}$ is the pseudo-inverse of $\mathbf{A}$. The azimuth angle of thruster $i$ is obtained by its components $T_{xi}$ and $T_{yi}$. An azimuth filtering was introduced to prevent the thruster from tear and wear and a maximum azimuth rotation velocity of $9^o$/s was assumed.

An extra feature is included in the algorithm in order to cope with situations leading to singular problems. These problems can arise whenever a small thrust is required perpendicular to the instantaneous direction of the total thrust provided by all propellers which, due to azimuth filtering, cannot adjust their directions in time. This situation occurs whenever matrix $\mathbf{A}$ presents a singular value close to zero.

## APPENDIX B– FEEDBACK LINEARIZATION CONTROL

Rewriting Eq.(1) in terms of the accelerations and velocities in the OXY fixed coordinate system, being R the reference point that lays in the center line of the barge, $x_R$ ahead the midship section, one can easily obtain:

$$\begin{pmatrix} \ddot{X}_R \\ \ddot{Y}_R \\ \ddot{\psi} \end{pmatrix} = \begin{pmatrix} f_{X,din}(\dot{\mathbf{X}}_\mathbf{R}) \\ f_{Y,din}(\dot{\mathbf{X}}_\mathbf{R}) \\ f_{\psi,din}(\dot{\mathbf{X}}_\mathbf{R}) \end{pmatrix} + \mathbf{C}(\psi) \begin{pmatrix} F_{1RE} + F_{1RO} + F_{1RT} \\ F_{2RE} + F_{2RO} + F_{2RT} \\ F_{6RE} + F_{6RO} + F_{6RT} \end{pmatrix} \qquad (7)$$

where $f_{i,din}$ are functions of the inertial properties of the barge and its velocity, $\mathbf{C}$ is a rotation matrix depending on the yaw angle and $F_{iR}$ are the forces transferred to the reference point.

Assuming that all terms in Eq.(7) are accurately known, the feedback linearization controller that guarantees that the states follows the desired ones ($X_D$, $Y_D$, $\Psi_D$) is given by:

$$\begin{pmatrix} F_{1RT} \\ F_{2RT} \\ F_{6RT} \end{pmatrix} = -\mathbf{C}^{-1} \begin{pmatrix} \hat{f}_{X,din}(\dot{\mathbf{X}}_\mathbf{R}) \\ \hat{f}_{Y,din}(\dot{\mathbf{X}}_\mathbf{R}) \\ \hat{f}_{\psi,din}(\dot{\mathbf{X}}_\mathbf{R}) \end{pmatrix} - \begin{pmatrix} \hat{F}_{1RE} + \hat{F}_{1RM} \\ \hat{F}_{2RE} + \hat{F}_{2RM} \\ \hat{F}_{6RE} + \hat{F}_{6RM} \end{pmatrix} + \mathbf{C}^{-1} \begin{pmatrix} \ddot{X}_D - 2l_X \dot{\tilde{X}} - l_X{}^2 \tilde{X} \\ \ddot{Y}_D - 2l_Y \dot{\tilde{Y}} - l_Y{}^2 \tilde{Y} \\ \ddot{\psi}_D - 2l_\psi \dot{\tilde{\psi}} - l_\psi{}^2 \tilde{\psi} \end{pmatrix} \qquad (8)$$

where (~) denotes the tracking error and (^) the best "estimate" of the corresponding term. The control parameters $l$ are related to the bandwidth of the closed loop system. It is recommended to keep them smaller either than non-modeled resonant modes or than the inverse of phase lags of the system.